Chiral d-wave RVB state on honeycomb lattice as a generalized staggered flux phase

Tao Li
Department of Physics, Renmin University of China, Beijing 100872, P.R.China
(Dated: July 20, 2011)

We show the chiral d-wave RVB state on honeycomb lattice stands as a natural generalization of the staggered flux phase on square lattice. Although the state is generated from a time reversal symmetry broken mean field ansatz, it actually represents a fully symmetric spin liquid state with a positive definite wave function in the sense of Marshall sign rule for unfrustrated antiferromagnets. The evolution of the state with the parameter Δ/χ follows exactly the same manner as that of the staggered flux phase on square lattice. The critical pairing strength corresponding to the π-flux phase is found to be $\Delta/\chi = \sqrt{2}$. As a result of the geometric frustration between neighboring plaquette on honeycomb lattice, a direct generalization of the $U(1)$ staggered flux pattern on square lattice to honeycomb lattice is impossible. Replacing it is the chiral d-wave state with Z_2 gauge structure. However, this Z_2 gauge structure is found to be ineffective after Gutzwiller projection and the system does not support topological degeneracy. The chiral d-wave RVB state is also found to be a rather good variational state for the Heisenberg model on honeycomb lattice. The spin correlation of the chiral d-wave state is found to be greatly enhanced as compared to the mean field prediction.

PACS numbers: 75.10.Kt,71.27.+a

I. INTRODUCTION

The study of correlated electrons on honeycomb lattice has attracted much interest recently. The honeycomb lattice has the smallest possible coordinate number of 3 for a two dimensional lattice and hosts Dirac-type dispersion at half filling. It is interesting to understand how the electron correlation effect will manifest itself in such a background.

A comparison with the square lattice case is of particular interest. Both lattices are bipartite and the antiferromagnetic long range order is unfrustrated in the strongly correlated limit. However, at half filling, the honeycomb lattice has a Dirac-type dispersion and a finite correlation strength is needed to induce antiferromagnetic order on honeycomb lattice, while on square lattice, the system form antiferromagnetic long range order immediately as we turn on interaction as the half filled system has a nested Fermi surface. More recently, it is discovered that the transition from the semimetal phase to the antiferromagnetic ordered state on honeycomb lattice may take place in a two step manner, leaving a small but finite intermediate correlation range in which the system may enter a spin liquid state with unconventional characteristics[1].

On square lattice, the antiferromagnetic order is destroyed by charge carrier doping. The resultant state is believed to have d-wave superconducting pairing and may be responsible for the superconductivity of the high-T_c cuprates. What is the analogy of these doping effect for the correlated electron system on honeycomb lattice? More specifically, what is the pairing symmetry of the resultant superconducting state, provided that the doped system does enter some kind of unconventional superconducting state. This inquire is even more attractive on honeycomb lattice than on square lattice, as the undoped honeycomb system already show signature of spin liquid ground state, which is nothing but a undoped version of the pairing state, the RVB state.

Superconductivity on system with a honeycomb lattice, especially that on graphene, has been studied by many researchers from both theoretical and experimental perspectives[2–9]. However, in most of these studies, the electron correlation effect does not play an essential role and the related pairing state has either s-wave or extended s-wave pairing symmetry, originated from exchanging phonon or other excitations. When the electron correlation effect is taken into account, the chiral d-wave pairing state[6, 9] has been proposed as a generalization of the d-wave pairing state on square lattice to honeycomb lattice(see Fig.1). However, it is not clear how the time reversal symmetry broken chiral state are connected to the antiferromagnetic ordered state at half filling.

At this point, it is quite useful to recall how the pairing symmetry of the superconducting state is determined in the strong correlation limit on square lattice. Here, a RVB state called staggered flux phase is found to be the best variational state at half filling in the restricted space of Fermionic RVB state[10–13], although it is known that the half filled system inevitably has an antiferromagnetic long range order. The staggered flux phase has the virtue that the antiferromagnetic short range correlation is greatly improved by the introduction of a non zero staggered flux. Up to a SU(2) gauge transformation, the introduction of the staggered flux is found to be equivalent to the introduction of d-wave pairing between the Fermionic spinons, especially, when the pairing and hoping order parameter becomes identical, the staggered flux becomes π. For general value of the staggered flux, the pairing amplitude and the flux is related by the rela-

tion $\tan\frac{\phi}{4}=\frac{\Delta}{\chi}$. It is thus quite natural that the doped system will choose the d-wave pairing state as its superconducting state as the antiferromagnetic superexchange is already optimized by the staggered flux.

Thus, a natural questions arises as what is the analog of the staggered flux phase on the honeycomb lattice, which can hopefully improve the superexchange interaction by some kind of pairing(flux). However, except for the π-flux phase, a naive generalization the staggered flux pattern for general flux value to the honeycomb lattice is impossible as a result of the geometric frustration between the neighboring hexagonal plaquette(see Fig. 2). Such a difference with square lattice originates from the frustrated nature of the dual lattice of the honeycomb lattice, which is the triangular lattice. Thus a generalization of the staggered flux phase to honeycomb lattice in the space of $U(1)$ staggered flux is impossible. However, generalization of the staggered flux phase in the larger space of $SU(2)$ flux is still possible. In this paper, we show that the RVB state with chiral d-wave pairing just fit such a need.

More specifically, we show that the chiral d-wave RVB state on honeycomb lattice can be taken as a generalized staggered flux phase. It actually describes a spin liquid state with the full symmetry of the Heisenberg model on honeycomb lattice and evolves in exactly the same way as the staggered flux phase on square lattice as a function of the parameter Δ/χ(see Fig.3). When $\frac{\Delta}{\chi}=0$, the state reduces to the uniform RVB state on honeycomb lattice, which has Dirac-type spinon dispersion. When $\frac{\Delta}{\chi}=\sqrt{2}$, the state is gauge equivalent to the π flux phase on the honeycomb lattice. When $\frac{\Delta}{\chi}$ exceed $\sqrt{2}$ and approaches infinite, the state again evolves back to the uniform RVB state with zero flux. It is interesting to note that in an earlier work on symmetric spin liquid state on honeycomb lattice, the chiral d-wave RVB state is classified to be a Z_2 spin liquid in the neighborhood of the uniform RVB state[14]. As its cousin on square lattice, the introduction of the staggered flux improves the antiferromagnetic correlation and we find the chiral d-wave RVB state stands as a rather good variational state for the Heisenberg model on honeycomb lattice. Unlike the staggered flux phase on square lattice, for general flux value, the mean field ansatz for the chiral d-wave RVB state posses a Z_2 rather than $U(1)$ gauge structure. We also find that as a result of the bipartite nature of the lattice, both the staggered flux phase on square lattice and the chiral d-wave RVB state on honeycomb lattice satisfy the Marshall sign rule for unfrustrated antiferromagnet. Such sign structure will prohibit the system to show topological degeneracy in the Z_2 sense, no matter what is the gauge structure of the mean field ansatz for the RVB state.

This paper is organized as follows. In the next two sections, we will review some well known results about the RVB state in general and the staggered flux phase on square lattice in particular to set up the stage for our discussion. In section IV, we present our results for the chiral d-wave RVB state. Section V contains a detailed comparison between the staggered flux phase on square lattice and the chiral d-wave RVB state on honeycomb and a discussion of some related issues.

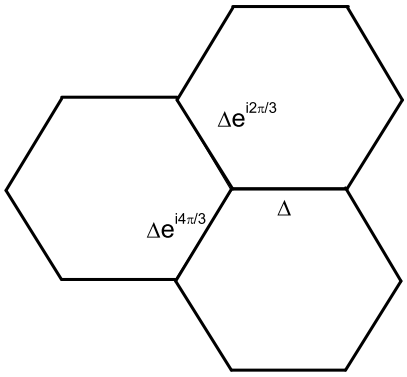

FIG. 1: The phases of the pairing potentials in the chiral d-wave RVB state on honeycomb lattice.

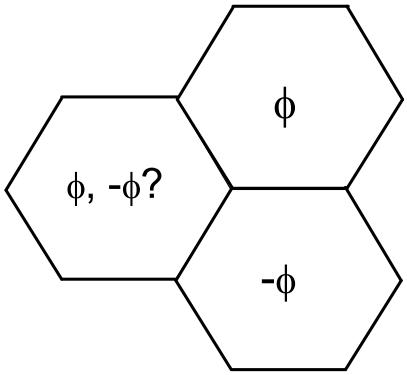

FIG. 2: The geometric frustration of $U(1)$ staggered flux on the honeycomb lattice.

II. RVB STATES AND THEIR GAUGE STRUCTURES

The RVB states studied in this paper are those derived form Gutzwiller projection of BCS-type mean

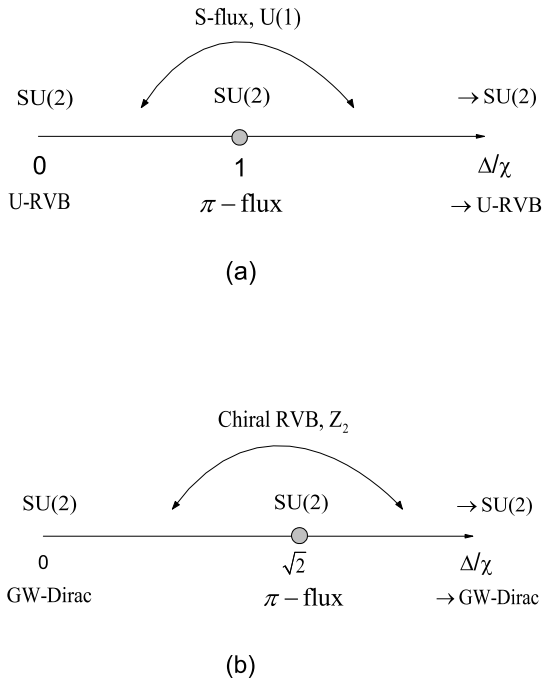

FIG. 3: The evolution of the gauge structure for the staggered flux phase on square lattice(a) and the chiral d-wave RVB state on honeycomb lattice(b). Here GW-Dirac denotes the uniform RVB state on honeycomb lattice, which has a Dirac-type spinon dispersion.

field ground state of the following general mean field ansatz[13]

$$\mathrm{H} = -\sum_{\langle i,j\rangle,\sigma}(\chi_{j,i}c^{\dagger}_{i,\sigma}c_{j,\sigma}+h.c.)+\sum_{\langle i,j\rangle,\sigma}(\Delta_{i,j}\sigma c^{\dagger}_{i,\sigma}c^{\dagger}_{j,\bar{\sigma}}+h.c.), \tag{1}$$

in which $\bar{\sigma}=-\sigma$, $\chi_{i,j}=\chi^{*}_{j,i}$ and $\Delta_{i,j}=\Delta_{j,i}$. Eq.(1) can also be taken as the saddle point approximation of a field theoretical description of the RVB state, in which $\chi_{i,j}$ and $\Delta_{i,j}$ are interpreted as two types of RVB order parameters. In the field theoretical formulation, the Gutzwiller projection into the subspace of no double occupancy amounts to integrating over the time component of the gauge fluctuation.

It is important to note that within the subspace of no double occupancy, a description of the RVB state in terms of $\chi_{i,j}$ and $\Delta_{i,j}$ becomes redundant as a result of the gauge degree of freedom in the mean field ansatz[13]. Such redundancy is accompanied by an underlying gauge structure of the RVB state so constructed. To see more clearly, it is better to rewrite the mean field ansatz in the Nambu form

$$\mathrm{H}=\sum_{\langle i,j\rangle}\psi^{\dagger}_{i}U_{i,j}\psi_{j}, \tag{2}$$

in which $\psi^{T}_{i}=(c_{i,\uparrow},c^{\dagger}_{i,\downarrow})$ is a two component spinor. $U_{i,j}=\begin{pmatrix}-\chi^{*}_{i,j} & \Delta_{i,j}\\ \Delta^{*}_{i,j} & \chi_{i,j}\end{pmatrix}$ is a 2×2 matrix. It is clear then that the system is invariant under the following $SU(2)$ gauge transformation

$$\begin{aligned}\psi_{i} &\rightarrow W_{i}\psi_{i}\\ U_{i,j} &\rightarrow W_{i}U_{i,j}W^{\dagger}_{j},\end{aligned} \tag{3}$$

in which W_i is a site-dependent $SU(2)$ matrix. As only the $SU(2)$ gauge singlet survive the Gutzwiller projection, $U_{i,j}$ and $W_iU_{i,j}W^{\dagger}_{j}$ actually describes the same RVB state.

Although $U_{i,j}$ is not gauge invariant and thus unphysical, it does contains important gauge invariant information on the structure of the RVB state. To uncover such internal gauge structure of the RVB state, it is a common practice to construct the loop operators[15], $P_i(C)=U_{i,j}U_{j,k}U_{k,l}\cdots U_{m,i}$, in which i denotes the starting point of the loop C and $j,k,\cdots m$ are the remaining sites along the loop. Under the $SU(2)$ gauge transformation, a loop operator transform as $P_i(C)\rightarrow W_iP_i(C)W^{\dagger}_{i}$ and thus its trace form a gauge invariant quantity. A RVB state is called to have $SU(2)$ gauge structure if all loop operator are proportional to the identity matrix $\tau_0=\begin{pmatrix}1 & 0\\ 0 & 1\end{pmatrix}$. Otherwise, it is called to have a $U(1)$ gauge structure if all $P_i(C)$ starting from any given site i commute with each other. If there are more than two loop operators starting from the same site do not commute with each other, the RVB state is called to have Z_2 gauge structure. The gauge structure of the RVB state is closely related to the existence of soft gauge mode in the long wave length limit in the effective field theoretic description of the RVB state. For example, if the gauge structure of the RVB state is $SU(2)$, then there will be $SU(2)$ soft gauge mode in the long wave length limit. While if the gauge structure of RVB state is Z_2, then there is no soft gauge mode at all in the long wave length limit. In such a case, the predictions made at the level of saddle point approximation is believed to be more reliable than those cases in which the RVB state has a $U(1)$ or $SU(2)$ gauge structure. In addition, the system with Z_2 gauge structure is argued in the effective field theory to support topological order and topological degeneracy - existence of degenerate ground states that can not be differentiated from any local probe[15].

The RVB state is generated from Gutzwiller projection of the BCS-type mean field ground state

$$|\mathrm{RVB}\rangle=\mathrm{P_G}|\mathrm{BCS}\rangle. \tag{4}$$

Such a state can in general be rewritten in the form of condensed spin singlet pairs

$$|\mathrm{RVB}\rangle=\mathrm{P_G}\left(\sum_{i,j}a(i-j)c^{\dagger}_{i,\uparrow}c^{\dagger}_{j,\downarrow}\right)^{\frac{N}{2}}|0\rangle, \tag{5}$$

in which $a(i-j)$ is the so called RVB amplitude and satisfy the relation $a(i-j)=a(j-i)$, N is the number of lattice site. As gauge equivalent mean field ansatz $U_{i,j}$ lead to identical RVB state, a RVB state is said to be symmetric if and only if the new ansatz after symmetry transformation is gauge equivalent to the old one. The projective symmetry group(PSG) provides a convenient scheme to classify the symmetric RVB state[15].

For RVB state with Z_2 gauge structure, which is argued to posses topological degeneracy from effective field theory, a Z_2 topological excitation called vison can be constructed by reversing the sign of RVB amplitude on bonds that crossing a branch cut line originated from the center of the vison an odd number of times. The topological nature of the vison excitation can be seen from the fact it acts as a π flux tube located at its origin for spinon traveling around it. Especially, when the RVB state is defined on a torus and a vison is trapped in one of the holes of the torus, one is left with a state that globally distinct from, but locally indistinguishable(and thus degenerate in the thermodynamic limit) from the original RVB state. This is nothing but the topological degeneracy. However, on bipartite lattice, the topological degeneracy predicted by the effective field theory can be lifted as a result of some special phase structure on the RVB state.

The detection of the Z_2 topological degeneracy is simplified by the fact that trapping a vison in the holes of the torus is gauge equivalent to change to boundary condition from periodic to anti-periodic or vice versa in the mean field ansatz[16, 17]. Thus to see if a particular RVB state does posses topological degeneracy in practice, we only need to calculate the overlap between RVB states generated from mean field ansatz with different boundary conditions around the holes of the torus and extrapolate the result to the thermodynamic limit. If the overlap extrapolate to zero in the thermodynamic limit, then the RVB state is said to posses topological degeneracy.

III. THE STAGGERED FLUX PHASE ON SQUARE LATTICE

The staggered flux phase(or d-wave RVB state) on square lattice plays a very important role in our understanding of the high-T_c superconductivity in cuprates. In the following we will review briefly some of the most important properties of this state[13] for a comparison with the chiral d-wave RVB state on honeycomb lattice.

The staggered flux phase on square lattice is generated from the following mean field ansatz

$$\mathrm{H_{SF}} = -\sum_{\langle i,j\rangle,\sigma}(e^{i\phi_{i,j}}c^\dagger_{i,\sigma}c_{j,\sigma}+h.c.), \tag{6}$$

in which the phase factor $\phi_{i,j}$ is introduced to guarantee that each plaquette of the square lattice is threaded by a $U(1)$ flux of value $\pm\Phi$ arranged in a staggered pattern. Although the mean field ansatz breaks the time reversal symmetry for general value of Φ, it is well known that the staggered flux phase is gauge equivalent to the d-wave RVB state generated from the following time reversal symmetric d-wave BCS mean field ansatz

$$\begin{aligned}\mathrm{H_{d-BCS}} = & -\chi\sum_{\langle i,j\rangle,\sigma}(c^\dagger_{i,\sigma}c_{j,\sigma}+h.c.) \\ & +\sum_{\langle i,j\rangle,\sigma}(\Delta_{i,j}c^\dagger_{i,\sigma}c^\dagger_{j,\bar\sigma}+h.c.),\end{aligned} \tag{7}$$

in which $\Delta_{i,j}=\pm\Delta$ for nearest neighboring sites i and j in the x/y direction. Here both χ and Δ are real and is determined from Φ by

$$\tan\frac{\Phi}{4}=\frac{\Delta}{\chi}. \tag{8}$$

In the following, we will use the d-wave gauge.

A. Mean field description

The spinon excitation spectrum in the staggered flux phase has the Dirac-type linear dispersion and is given by $E_\mathrm{k}=\sqrt{(\epsilon_\mathrm{k})^2+(\Delta_\mathrm{k})^2}$, in which $\epsilon_\mathrm{k}=-2\chi(\cos\mathrm{k}_x+\cos\mathrm{k}_y)$, $\Delta_\mathrm{k}=2\Delta(\cos\mathrm{k}_x-\cos\mathrm{k}_y)$. The nodes are located at $(\mathrm{k}_x,\mathrm{k}_y)=(\pm\pi/2,\pm\pi/2)$. As we will be concerned with the spin structure factor of the RVB state below, we present the mean field prediction for it here. The spin structure factor is defined as

$$S(\mathrm{q})=\frac{1}{N^2}\sum_{i,j}e^{i\mathrm{q}\cdot(i-j)}\langle S_i\cdot S_j\rangle. \tag{9}$$

The spin structure factor in a BCS mean field ground state is given by

$$S(\mathrm{q})=\frac{3}{8N^2}\sum_{\mathrm{k}}(1-\frac{\epsilon_\mathrm{k}\epsilon_{\mathrm{k+q}}+\Delta_\mathrm{k}\Delta_{\mathrm{k+q}}}{E_\mathrm{k}E_{\mathrm{k+q}}}). \tag{10}$$

Since the square lattice is bipartite and $\epsilon_\mathrm{k}=-\epsilon_{\mathrm{k+Q}}$, $\Delta_\mathrm{k}=-\Delta_{\mathrm{k+Q}}$ for $\mathrm{Q}=(\pi,\pi)$, we find $S(\mathrm{Q})=\frac{3}{4N}$ in the mean field theory. The spin structure factor is thus independent of the value of the staggered flux in the mean field theory. It also extrapolates to zero in the thermodynamic limit.

B. Gauge structure

The loop operator around the elementary plaquette of the square lattice in the staggered flux phase is given by

$$\begin{aligned}P_1(C) &= U_xU_yU_xU_y \\ &= (\chi^2-\Delta^2)^2-4\chi^2\Delta^2+4i\chi\Delta(\chi^2-\Delta^2)\tau_2,\end{aligned}$$

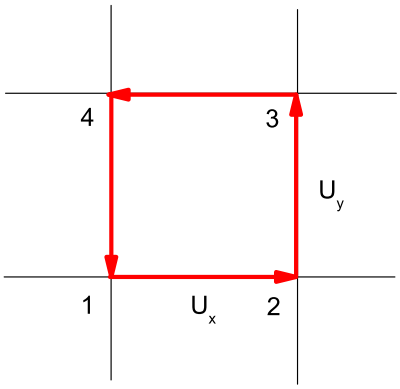

FIG. 4: The loop operator defined on the elementary plaquette of square lattice.

in which $U_x = -\chi\tau_3 + \Delta\tau_1$, $U_y = -\chi\tau_3 - \Delta\tau_1$. Here τ_1, τ_2 and τ_3 denote the three Pauli matrixes in the internal $SU(2)$ space.

When $\Delta/\chi = 0$, $|\Delta| = |\chi|$ or $\chi/\Delta = 0$, the loop operator is proportional to τ_0(here we assume that χ and Δ satisfy the normalization condition $\chi^2 + \Delta^2 = 1$). By induction we can show that all loop operators are proportional to τ_0 at these three points. The state with $\chi/\Delta = 0$ and that with $\Delta/\chi = 0$ are in fact gauge equivalent and is the well known uniform RVB state on square lattice. The state with $|\Delta| = |\chi|$ is the so called π-flux phase on square lattice. Thus, both the uniform RVB state and the π-flux phase posses a $SU(2)$ gauge structure. For general value of the staggered flux, the loop operator is not proportional to τ_0 and gauge structure can be shown to be $U(1)$. The evolution of the gauge structure with Δ/χ in the staggered flux phase is summarized in Fig.3(a).

C. Symmetries

The staggered flux actually respects all the physical symmetries of the Heisenberg model on square lattice. While translational symmetry and inversion symmetry is manifest in the d-wave gauge, the four-fold lattice rotational symmetry can be shown as follows.

Under the four-fold lattice rotation, the mean field ansatz transform as follows: $\chi \to \chi$, $\Delta \to -\Delta$. A global $SU(2)$ gauge transformation with $W_j = i\tau_3$ suffices to recover the original ansatz. The rotated ansatz and the original ansatz thus describe the same RVB state. This prove the rotational symmetry of the staggered flux phase.

The four-fold rotational symmetry of the staggered flux also implies the gauge equivalence between the state with staggered flux Φ and $-\Phi$. As the gauge flux is defined modula 2π, the state with staggered flux Φ and $2\pi-\Phi$ are gauge equivalent. In the d-wave gauge, this indicates that the state with $\Delta/\chi = a$ and the state with $\Delta/\chi = 1/a$ are gauge equivalent.

D. Sign structure of the staggered flux phase and topological degeneracy

In an Ising basis for the spins, the staggered flux phase can be expanded as follows

$$|\mathrm{SF}\rangle = \sum_{\{\sigma_i\}} \psi(\{\sigma_i\})|\{\sigma_i\}\rangle, \tag{11}$$

in which $|\{\sigma_i\}\rangle = |\sigma_1, \cdots, \sigma_N\rangle$ denotes an Ising basis. Then the wave function $\psi(\{\sigma_i\})$ can be shown to be real and satisfy the Marshall sign rule[17, 19] for unfrustrated antiferromagnet, namely, the sign of ψ is given by $(-1)^{N^{A\downarrow}}$, with $N^{A\downarrow}$ denoting the number of down spins in A sublattice.

Although the mean field ansatz of the staggered flux phase has at least a $U(1)$ gauge structure, it is still possible to construct a state with a trapped vison in the holes of a torus and check its orthogonality with the state with no trapped vison. Such a calculation has been done in previous studies[16] and it was found that the overlap extrapolates to a finite value in the thermodynamic limit, indicating no topological degeneracy for the staggered flux phase. This result is claimed to be a strong support of the effective field theory argument. However, a later investigation[17] indicates that the Marshall sign rule satisfied by the staggered flux phase plays a more essential role in removing the topological degeneracy.

E. Variational energy and spin structure factor

Both the short range and the long range spin correlation are seen to reach extreme at the uniform RVB state and the π-flux phase. This is a result of the gauge equivalence between states with staggered flux Φ and $-\Phi$ and that between states with staggered flux Φ and $2\pi - \Phi$, from which one can easily show that the spin correlation function should reach their extreme in the uniform RVB state and the π-flux phase.

The correlation between spins on nearest neighboring sites, $\frac{1}{2N}\sum_{\langle i,j\rangle}\langle S_i \cdot S_j\rangle$, which is proportional to the variational energy for the Heisenberg model on square lattice, is presented in Fig.5 as a function of Δ/χ. The optimal value for Δ/χ is found to be about 0.3. The variational energy reaches local maximum in both the uniform RVB state and the π-flux phase.

To probe the long range spin correlation, we have calculated the spin structure factor of the staggered flux

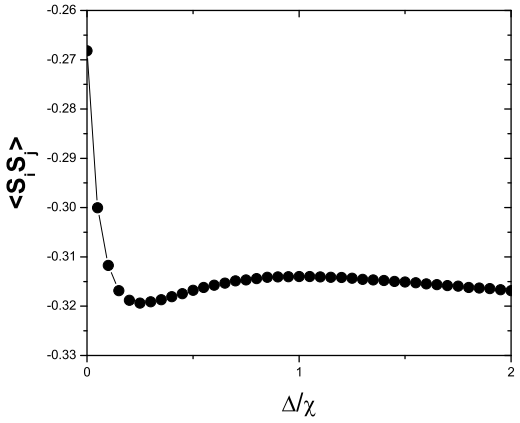

FIG. 5: The variational energy per bond calculated for the Heisenberg model on square lattice as a function of Δ/χ. The calculation is done on a 16×16 lattice with periodic-antiperiodic boundary condition. The error bars are smaller than the size of the symbols.

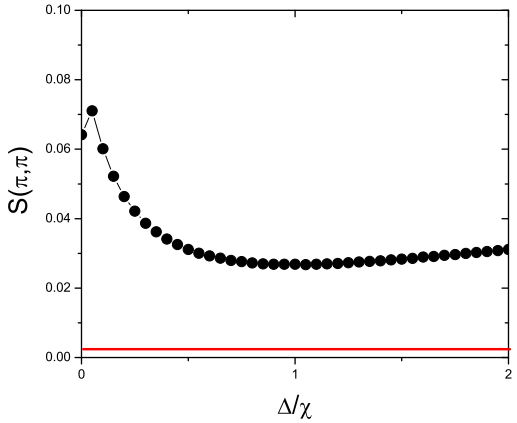

FIG. 6: The spin structure factor at $q = (\pi, \pi)$ as a function of Δ/χ for the staggered flux phase on square lattice. The calculation is done on a 16×16 lattice with periodic-antiperiodic boundary condition. The error bars are smaller than the size of the symbols.The red line denotes the mean field prediction, which is independent of Δ/χ.

phase. The spin structure factor peaks at the antiferromagnetic ordering wave vector $Q = (\pi, \pi)$. In Fig.6, we present the result for $S(Q)$ as a function of Δ/χ. The spin structure factor decrease monotonically with the staggered flux for $\Phi < \pi$. The small peak close to the uniform RVB state is a finite size effect and it moves toward the uniform RVB state with increasing lattice size and disappears in the thermodynamic limit.

In a recent work[20], we have shown that the uniform RVB state on square lattice actually describe a state with antiferromagnetic long range order as a result of the nested spinon Fermi surface. The spin structure factor follows the $S(Q) \approx S_0 + \alpha(1/L)^{5/4}$ behavior as a function of the linear scale of the lattice, L. While in the π-flux phase, $S(Q)$ is found to follow the $S(Q) \approx (1/L)^{3/2}$ behavior and no magnetic order is detected. In between the two extremes, the staggered flux has no magnetic long range order and the spin correlation function decay algebraically with distance with an exponent depending on the value of the staggered flux. Thus the uniform RVB state state on square lattice is an isolated singular point.

IV. THE CHIRAL D-WAVE RVB STATE ON HONEYCOMB LATTICE

The chiral d-wave RVB state on honeycomb lattice is generated from the following BCS mean field ansatz

$$\mathrm{H_{BCS}} = -t \sum_{\langle i,j\rangle,\sigma} (c^\dagger_{i,\sigma} c_{j,\sigma} + h.c.) + \sum_{\langle i,j\rangle,\sigma} \Delta_{i,j} (\sigma c^\dagger_{i,\sigma} c^\dagger_{j,\bar{\sigma}} + h.c.), \tag{12}$$

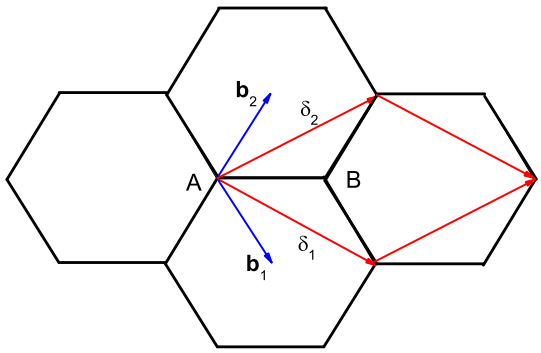

FIG. 7: The unit cell of the honeycomb lattice.

in which $\sum_{\langle i,j\rangle}$ denotes sum over nearest neighboring sites on honeycomb lattice. $\Delta_{i,j}$ denotes the pairing order parameter between site i and j. In the chiral d-wave RVB state, $\Delta_{i,j}$ is a complex number and the phase of $\Delta_{i,j}$ in the three directions differ with each other by $\pm\frac{2\pi}{3}$(see Fig.1).

A. Mean field description

The mean field Hamiltonian for the chiral d-wave state can be easily diagonalized in momentum space in which

it takes the form

$$\mathrm{H_{BCS}} = \sum_{\mathrm{k}} \psi^{\dagger}_{\mathrm{k}} \mathrm{M} \psi_{\mathrm{k}}, \tag{13}$$

in which ψ_{k} is a four component spinor given by $\psi^T_{\mathrm{k}} = (c^A_{\mathrm{k}\uparrow}, c^B_{\mathrm{k}\uparrow}, c^{A\dagger}_{-\mathrm{k}\downarrow}, c^{B\dagger}_{-\mathrm{k}\downarrow})$. Here A and B are sublattice index. The 4×4 matrix M is given by

$$\mathrm{M} = \begin{pmatrix} 0 & \gamma_{\mathrm{k}} & 0 & \Delta_{\mathrm{k}} \\ \gamma^*_{\mathrm{k}} & 0 & \Delta_{-\mathrm{k}} & 0 \\ 0 & \Delta^*_{-\mathrm{k}} & 0 & -\gamma_{\mathrm{k}} \\ \Delta^*_{\mathrm{k}} & 0 & -\gamma^*_{\mathrm{k}} & 0 \end{pmatrix}, \tag{14}$$

in which $\gamma_{\mathrm{k}} = (1 + e^{-i\mathrm{k}\cdot\delta_1} + e^{-i\mathrm{k}\cdot\delta_2})$, $\Delta_{\mathrm{k}} = \Delta(1 + e^{i\frac{2\pi}{3}} e^{-i\mathrm{k}\cdot\delta_1} + e^{i\frac{4\pi}{3}} e^{-i\mathrm{k}\cdot\delta_2})$. Here δ_1 and δ_2 are the two lattice translational vectors of the honeycomb lattice(see Fig.7).

The eigenvalues of the Hamiltonian are given by

$$\mathrm{E}^2_{\mathrm{k}\pm} = \gamma^2_{\mathrm{k}} + \frac{|\Delta_{\mathrm{k}}|^2 + |\Delta_{-\mathrm{k}}|^2 \pm \sqrt{(|\Delta_{\mathrm{k}}|^2 - |\Delta_{-\mathrm{k}}|^2)^2 + 4|g_{\mathrm{k}}|^2}}{2}, \tag{15}$$

in which $g_{\mathrm{k}} = \gamma_{-\mathrm{k}}\Delta^*_{-\mathrm{k}} - \gamma_{\mathrm{k}}\Delta^*_{\mathrm{k}}$.

When $\Delta = 0$, the dispersion reduces to that of the Dirac Fermion, $\mathrm{E_k} = \pm|\gamma_{\mathrm{k}}|$. At $(k_1, k_2) = \pm(2\pi/3, -2\pi/3)$, $\mathrm{E_k} = 0$. Here we have used the convention that $\mathrm{k} = k_1\mathbf{b}_1 + k_2\mathbf{b}_2$ for the momentum. $\mathbf{b}_1$ and $\mathbf{b}_2$ are the two reciprocal vectors. They are dual to the lattice translational vectors δ_1 and δ_2 and satisfy the relation $\delta_i \cdot \mathbf{b}_j = \delta_{i,j}$.

When $(k_1, k_2) = \pm(2\pi/3, -2\pi/3)$, $\gamma_{\mathrm{k}} = 0$ and thus $g(\mathrm{k}) = 0$. It can also be shown that one of the two gap functions, Δ_{k} or $\Delta_{-\mathrm{k}}$, is zero at $(k_1, k_2) = \pm(2\pi/3, -2\pi/3)$. It is then easy to verify that the nodes at $(k_1, k_2) = \pm(2\pi/3, -2\pi/3)$ persist for any value of Δ. In addition, new nodes may emerge at nonzero Δ. In the appendix, we show the dispersion for some typical values of Δ/χ. It should be noted that the location of the additional nodes move continuously in the momentum space with Δ/χ.

On the honeycomb lattice, the spin structure factor at the antiferromagnetic ordering wave vector can be defined as follows

$$S(Q) = \frac{1}{N^2} \sum_{i,j} \langle (S^A_i - S^B_i) \cdot (S^A_j - S^B_j) \rangle. \tag{16}$$

From the mean field theory, it is straightforward (though somewhat tedious) to show that $S(Q)$ is independent of Δ/χ and is given by the $S(Q) = \frac{3}{4N}$. As for the staggered flux phase on square lattice, the Δ/χ independence of $S(Q)$ on honeycomb lattice at the mean field level is a result of the bipartite nature of the lattice.

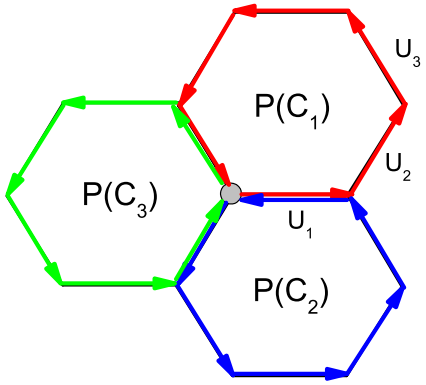

FIG. 8: The loop operators of the chiral d-wave RVB state on the elementary plaquette of the honeycomb lattice. The gray dots denotes the common starting point of the loop operators.

B. Gauge structure

From every sites of the honeycomb lattice, there are three elementary loop operators. They are given by

$$\begin{aligned} P(C_1) &= (U_1U_2U_3)^2 \\ P(C_2) &= (U_2U_3U_1)^2 \\ P(C_3) &= (U_3U_1U_2)^2, \end{aligned} \tag{17}$$

in which $U_1 = -\chi\tau_3 + \Delta\tau_1 = \rho u_1$, $U_2 = -\chi\tau_3 - \frac{\Delta}{2}\tau_1 + \frac{\sqrt{3}\Delta}{2}\tau_2 = \rho u_2$, $U_3 = -\chi\tau_3 - \frac{\Delta}{2}\tau_1 - \frac{\sqrt{3}\Delta}{2}\tau_2 = \rho u_3$ are RVB order parameters on bonds in three directions. $\rho = \sqrt{\chi^2 + \Delta^2}$ is the 'length' of the RVB order parameter. u_1, u_2, u_3 are three Hermitian matrix satisfying $u_1u_1 = u_2u_2 = u_3u_3 = \tau_0$. The products of U_1, U_2 and U_3 in Eq.17 are given by

$$\begin{aligned} U_1U_2U_3 &= -i\frac{3\sqrt{3}}{2}\chi\Delta^2 \\ &+ (\chi^2 - \frac{\Delta^2}{2})(-\chi\tau_3 + \Delta\tau_1 - \sqrt{3}\Delta\tau_2) \\ U_2U_3U_1 &= -i\frac{3\sqrt{3}}{2}\chi\Delta^2 \\ &+ (\chi^2 - \frac{\Delta^2}{2})(-\chi\tau_3 + \Delta\tau_1 + \sqrt{3}\Delta\tau_2) \\ U_3U_1U_2 &= -i\frac{3\sqrt{3}}{2}\chi\Delta^2 \\ &+ (\chi^2 - \frac{\Delta^2}{2})(-\chi\tau_3 - 2\Delta\tau_1). \end{aligned} \tag{18}$$

From Eq.18, it can be easily seen that at the three special points $\Delta = 0$, $\Delta = \sqrt{2}\chi$ and $\chi = 0$(with the normalization condition $\Delta^2 + \chi^2 = 1$ assumed), all the three loop operators are proportional to the identity matrix τ_0.

Sublattice/Parity	(o,o)	(o,e)	(e,o)	(e,e)
A	τ_0	$-iu_3$	$-iu_2$	$-iu_1$
B	$u_1\tau_3$	$-u_2\tau_3$	$-u_3\tau_3$	$i\tau_3$

TABLE I: The gauge transformation that relate the chiral d-wave RVB state with $\Delta/\chi = \sqrt{2}$ and the π-flux phase shown in Fig.9

By induction it can then be shown that all loop operators are proportional to τ_0. The system thus has $SU(2)$ gauge structure at these three special points. This is exactly what happens in the staggered flux phase on square lattice. In fact, it can further shown that the chiral RVB state on honeycomb lattice with $\Delta = 0$ ($\chi = 0$) and $\Delta = \sqrt{2}\chi$ are just the uniform RVB state and π-flux phase on honeycomb lattice.

The gauge equivalence between the state with $\Delta = 0$ and $\chi = 1$ ($U_1 = U_2 = U_3 = -\tau_3$) and that with $\chi = 0$ and $\Delta = 1$ ($U_1 = \tau_1$, $U_2 = -\frac{1}{2}\tau_1 + \frac{\sqrt{3}}{2}\tau_2$, $U_3 = -\frac{1}{2}\tau_1 - \frac{\sqrt{3}}{2}\tau_2$) can be shown by the following $SU(2)$ gauge transformation. First, the phase of the pairing order parameter in the state with $\chi = 0$ and $\Delta = 1$ can be gauged away by a $U(1)$ gauge transformation. After this $U(1)$ gauge transformation, the mean field ansatz takes the form $U_1 = U_2 = U_3 = \tau_1$. Then a uniform $SU(2)$ rotation with $W_i = e^{-i\frac{\pi}{4}\tau_2}$ suffices to transform the ansatz into the form $U_1 = U_2 = U_3 = -\tau_3$. Similarly, the gauge equivalence between the state with $\Delta = \sqrt{2}\chi$ and the π-flux phase on honeycomb lattice(see Fig.9) can be established with the $SU(2)$ gauge transformation given in Table.1 .

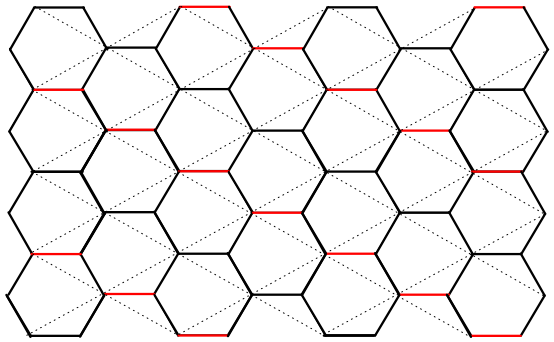

FIG. 9: The mean field ansatz for the π-flux on honeycomb lattice. The bonds in red have a negative hopping integral, while other bonds have a positive hopping integral.

For other value of Δ/χ, the three loop operators do not commute with each other and the system has a Z_2 gauge structure. This is quite different from the square lattice where the $SU(2)$ points are connected by intermediate state with $U(1)$ gauge structure. The origin of such a difference can be traced back to the geometric frustration in the dual lattice of honeycomb lattice. To see the evolution of the gauge structure more clearly, we rewrite the loop operator in the following form

$$\begin{aligned} P(C_1) &= -\rho^6 e^{i\Phi\vec{n}_1\cdot\vec{\tau}} \\ P(C_2) &= -\rho^6 e^{i\Phi\vec{n}_2\cdot\vec{\tau}} \\ P(C_3) &= -\rho^6 e^{i\Phi\vec{n}_3\cdot\vec{\tau}}, \end{aligned} \tag{19}$$

in which the absolute value of the gauge flux Φ is determined by

$$\cos\frac{\Phi}{2} = \frac{3\sqrt{3}\chi\Delta^2}{2\rho^3}. \tag{20}$$

$\vec{n}_1$, $\vec{n}_2$ and $\vec{n}_3$ are three vectors of unit length and are given by

$$\begin{aligned} \vec{n}_1 &= r(\Delta, -\sqrt{3}\Delta, -\chi) \\ \vec{n}_2 &= r(\Delta, \sqrt{3}\Delta, -\chi) \\ \vec{n}_3 &= r(-2\Delta, 0, -\chi), \end{aligned} \tag{21}$$

in which $r = 1/\sqrt{\chi^2 + 4\Delta^2}$. The three vectors form the equal angle with each other as shown schematically in Fig.10. When $\Delta = 0$, all the three vectors lies in the $-\tau_3$ direction. With increasing Δ/χ, the three vectors split from each other. When $\Delta/\chi \to \infty$, $\vec{n}_1$, $\vec{n}_2$ and $\vec{n}_3$ evolves into the $\tau_1 - \tau_2$ plane with a 120^0 angle between each other.

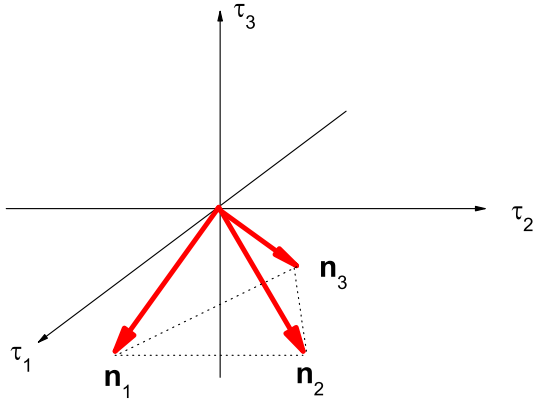

FIG. 10: The direction of the three loop operators in the internal $SU(2)$ gauge space.

The structure of the loop operators presented above can be viewed as a generalized staggered flux pattern on honeycomb lattice. The absolute value of the flux for the staggered flux phase on square lattice and the chiral d-wave RVB state on honeycomb lattice are both uniform. It is the direction of the flux that is responsible for its staggered character. On square lattice, where the dual lattice is also square lattice, a two sublattice (antiferromagnetic) arrangement of the direction of the flux is the

most natural choice. While on honeycomb lattice, where the dual lattice is triangular lattice, a three sublattice arrangement of the direction for the flux is more natural.

The discussion above on the gauge structure of the chiral d-wave RVB state is summarized in Fig.3b. Its similarity with the figure for the staggered flux phase on square lattice is apparent. It is for this reason that we call the chiral d-wave RVB state a generalized staggered flux phase on honeycomb lattice.

C. Symmetries

As will be clear below, the term 'chiral' is in fact not quite accurate. It can be shown that the time reversal symmetry breaking manifested in the mean field ansazt is in fact an artifact of the mean field description. In fact, it can be more generally proved that the chiral d-wave RVB state actually respects all the physical symmetries for the Heisenberg model on honeycomb lattice. The effect of the symmetry transformation on the mean field ansatz is to induce permutations between U_1, U_2 and U_3. Thus to prove the symmetry of the chiral d-wave RVB state it suffice to show that the RVB order parameters after such permutation are gauge equivalent to the original one.

For example, under the time reversal transformation, U_2 and U_3 are exchanged. Such a change can also be induced by the following two-step gauge transformation. First, we rotate the ansatz uniformly along the τ_2 axis by π. Then as the lattice is bipartite, we effect a $U(1)$ gauge transformation by π uniformly on sites in the B sublattice. This proves the time reversal symmetry of the chiral d-wave RVB state. Note that the bipartite nature of the lattice is essential for the restoration of the time reversal symmetry. Another example is provided by the $2\pi/3$ rotation of the lattice, which induces a cyclic exchange among U_1, U_2 and U_3. It can be easily shown that such a cyclic exchange can also be induced by a uniform rotation of the ansatz along the τ_3-axis in the $SU(2)$ space by an angle $2\pi/3$. This proves the rotational symmetry of the chiral d-wave RVB state.

We note that as the exchange between U_2 and U_3 and the cyclic exchange among U_1,U_2 and U_3 exhausts the generators of the permutation group of U_1,U_2 and U_3, we have in fact proved the full symmetry of the chiral d-wave RVB state.

D. Sign structure of the chiral d-wave RVB state and topological degeneracy

Beside being time reversal symmetric, it can also be shown that the chiral d-wave RVB state on honeycomb lattice actually has a positive definite wave function in the sense of Marshall sign rule for bipartite antiferromagnet, although the mean field ground state break the time reversal symmetry and has a complex valued wave function. This remarkable result is in fact a general property for all RVB states generated from bipartite mean field ansatz[17]. It is also argued that the Marshall sign structure will remove from the projected wave function the topological degeneracy, even if the mean field ansatz has a Z_2 gauge structure.

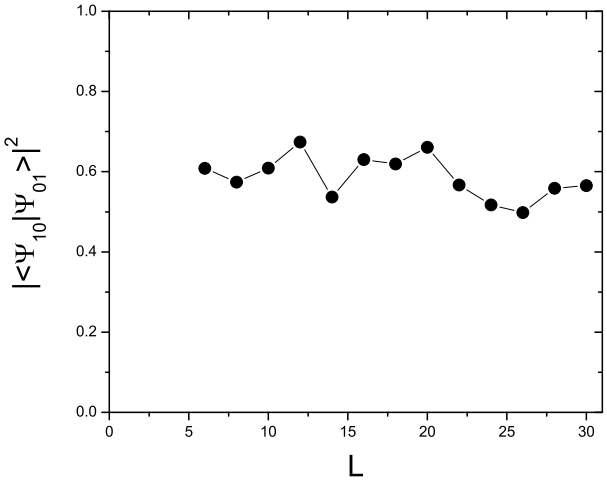

FIG. 11: The overlap between $|\Psi_{10}\rangle$ and $|\Psi_{01}\rangle$ on a $L\times L\times 2$ honeycomb lattice as a function of the lattice size L. The error bars are smaller than the size of the symbols. The oscillation of the curve is caused by the complex nodal structure of the chiral d-wave RVB state, which move continuously in the momentum space with Δ/χ.

The absence of the topological degeneracy on bipartite system can be argued as follows. As changing the boundary condition around the hole of a tours will not change the bipartite nature of the mean field ansatz, both the projected state with trapped vison and without trapped vison will be positive definite in the sense of Marshall sign rule. It is just this insensitivity of the sign structure to the trapped Z_2 gauge flux that is responsible for the absence of the topological degeneracy. In a recent work[21], we have shown through VMC that the chiral d-wave RVB state on honeycomb lattice does not support topological degeneracy. However, since the calculation is done in the region $\Delta/\chi < \sqrt{2}$, we would like to supplement it with the result in the region $\Delta/\chi > \sqrt{2}$.

The overlap between states with different number of vison in both holes of the torus for the chiral d-wave RVB state is shown in Fig.11. Here $|\Psi_{10}\rangle$ denotes the state with trapped vison in the hole surrounded by the x-circumference but no vison in the hole surrounded by the y-circumference. $|\Psi_{01}\rangle\rangle$ denotes the state with trapped vison in the hole surrounded by the y-circumference but no vison in the hole surrounded by the x-circumference. The calculation is done at $\Delta/\chi = 5$. The overlap is seen to oscillate with the lattice size. Such oscillation is caused by the complex nodal structure of the chiral d-wave RVB state, which move continuously in the momentum space

with Δ/χ. However, it is clear that the overlap will extrapolate to finite value in the thermodynamic limit.

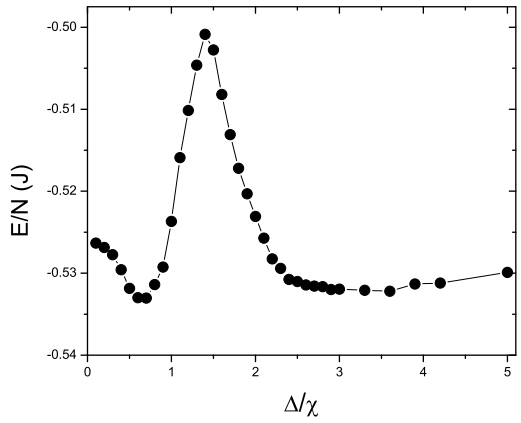

FIG. 12: The variational energy per site for the Heisenberg model on honeycomb lattice calculated from the chiral d-wave RVB state. The calculation is done on a $16\times16\times2$ lattice with periodic-antiperiodic boundary condition. The error bars are smaller than the size of the symbols.

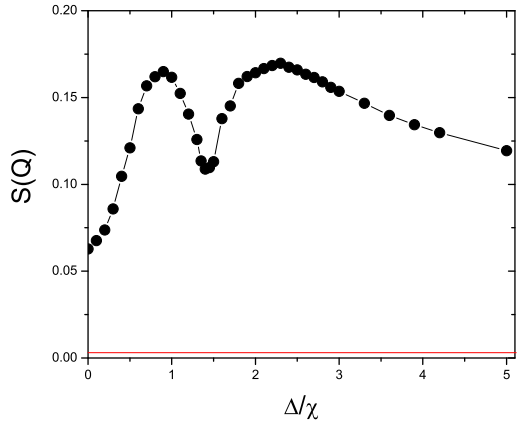

FIG. 13: The spin structure factor at the antiferromagnetic ordering wave vector for the chiral d-wave RVB state on honeycomb lattice as a function Δ/χ. The calculation is done on a $16 \times 16 \times 2$ lattice with periodic-antiperiodic boundary condition. The error bars are smaller than the size of the symbols. The small non-analycity of the curve is checked to be finite size effect induced by the moving nodes in the momentum space. The red line denotes the mean field prediction, which is independent of Δ/χ.

E. Variational energy and spin structure factor

The variational energy for the Heisenberg model on honeycomb lattice is shown in Fig.12 as a function of Δ/χ. As for the staggered flux phase on square lattice, the variational energy is optimized with a state intermediate between uniform RVB state and the π-flux phase. Unlike the square lattice case, the difference in energy between the uniform RVB state and the optimized variational state in this class of RVB state is seen to be small. As the exact ground state energy is estimated to be $-0.55J$ per site from exact diagonalizition studies[18], we see the chiral d-wave RVB state in fact represents a rather good variational state for the Heisenberg model on honeycomb lattice.

The spin structure factor at the antiferromagnetic ordering wave vector for the chiral d-wave RVB state is plotted in Fig.13 as a function of Δ/χ. As a comparison we also plot the value calculated from the mean field ground state($=\frac{3}{4N}$), which is independent of the pairing strength. The spin structure factor is seen to be reduced at the uniform RVB state and the π flux phase, both of which having a $SU(2)$ gauge structure at the mean field level. This can be taken as a evidence that the $SU(2)$ gauge fluctuation will reduce rather than enhance the spin correlation.

We have also calculated the size dependence of the spin structure factor at $\Delta/\chi = 0$, $\Delta/\chi = 1$ and $\Delta/\chi = \sqrt{2}$ to see how the gauge structure affects the spin correlation in the thermodynamic limit. The results are shown in Fig.14. We find in all of the three states the spin structure factor decay algebraically with the linear scale of the lattice, indicating no magnetic long range order in the thermodynamic limit. This is different from square lattice, where the uniform RVB state is found to posses antiferromagnetic long range order. A fit to the date with the formula $S(Q) = \alpha(1/L)^\beta$ shows that the exponent β varies with the value of Δ/χ. More specifically, the exponent at $\Delta/\chi = 0$ is found to be approximately 1.5. It is reduced to 1 at $\Delta/\chi = 1$ and return to 1.3 at $\Delta/\chi = \sqrt{2}$. Thus, a finite value for the flux will not only improve the local spin correlation, but also result in more long ranged spin correlation.

V. CONCLUSION

From the above discussion, we see the chiral d-wave RVB state on honeycomb lattice indeed stands as a natural generalization of the staggered flux phase on square lattice. The two states shares the following properties.

(1) Both states respect the full symmetry of the Heisenberg model on respective lattices and have a positive definite wave function in the sense of the Marshall sign rule.

(2) Both states evolves with Δ/χ in the same manner. With the increase of Δ/χ, both states evolve from the

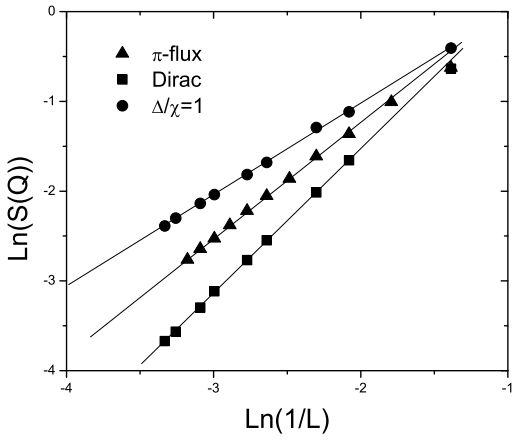

FIG. 14: The finite size scaling behavior of the spin structure factor of the chiral d-wave RVB state for $\Delta/\chi = 0$(Dirac), $\Delta/\chi = 1$ and $\Delta/\chi = \sqrt{2}$(π-flux).

uniform RVB state to the π-flux phase and then back to the uniform RVB state. The uniform RVB state and the π-flux phase on both lattices have a promoted gauge symmetry of $SU(2)$.

(3)The introduction of the gauge flux on both lattice improves the short range spin correlation and both the staggered flux phase on square lattice and the chiral d-wave RVB state on honeycomb lattice are rather good variational description of the Heisenberg model on respective lattices.

(4)As a result of the bipartite nature of the lattice and the resultant Marshall sign rule of the RVB state, both the staggered flux phase on square lattice and the chiral d-wave RVB state on honeycomb lattice do not support topological degeneracy, although the latter posses a Z_2 gauge structure at the saddle point level.

However, there are also important differences between the staggered flux phase on square lattice and the chiral d-wave RVB state on honeycomb lattice. The following is a list of the main differences.

(1)On square lattice, the intermediate state connecting the uniform RVB state and the π-flux phase has a $U(1)$ gauge structure. However, on honeycomb lattice, the two states are connected by intermediate state with Z_2 gauge structure. This difference originates from the frustrated nature of the dual lattice of honeycomb lattice. Related with this difference is the difference in the staggering pattern of the gauge flux on the two lattices. On square lattice, the gauge flux form a two sublattice collinear pattern. On the other hand, the gauge flux on the honeycomb lattice form a three sublattice non-collinear pattern.

(2)As a result of the non-collinear nature of the gauge flux in the chiral d-wave state, the states with gauge flux Φ below $\Delta/\chi = \sqrt{2}$ are not gauge equivalent to the states with gauge flux $2\pi - \Phi$ above $\Delta/\chi = \sqrt{2}$, except the special case of the uniform RVB state. Thus in principle the π-flux phase on honeycomb lattice need not be a extreme of physical properties as functions of Δ/χ, although we find both the variational energy and the spin structure factor do reach their extreme at the π-flux phase. On the other hand, on square lattice, the π-flux phase must be an extreme of physical properties as functions of Δ/χ as protected by the $\Phi \to 2\pi - \Phi$ symmetry.

(3)On square lattice, the uniform RVB state posses antiferromagnetic long range order. However, on honeycomb lattice, no magnetic order is detected in the uniform RVB state. This difference can be induced by the difference in their spinon dispersion. While the uniform RVB state on square lattice has a large and nested spinon Fermi surface, which is unstable toward antiferromagnetic ordering, the uniform RVB state on honeycomb lattice has an isotropic Dirac-type spinon dispersion, just as the π-flux phase on square lattice. Indeed, the spin structure factor of the uniform RVB state on honeycomb lattice is found to show the same scaling behavior as the π-flux phase on square lattice[22].

(4)Although the variational energy can be improved by introducing gauge flux on both square lattice and honeycomb lattice, the amount of improvement is quite different. On square lattice, the introduction of staggered flux will lead to a 15% improvement in the variational energy of the Heisenberg model. On the other hand, the same energy gain on honeycomb lattice is less than 2%. This difference can also be induced by the difference in the spinon dispersion on the two lattices.

As the staggered flux phase plays such a central role in our understanding of the high-Tc superconductivity in cuprates from the perspective of RVB theory, it is quite natural to expect that the chiral d-wave RVB state will play the similar role, if the doped honeycomb system in the strongly correlated regime does support some kind of superconductivity. After doping, the time reversal symmetry will be broken and the state will become truly chiral. A full gap will also be opened in the doped system, as can be shown by including a chemical potential term in Eq.(13). There will be many interesting issues concerning this novel superconducting state, especially on its topological properties. However, as the condensation energy is much smaller than system on square lattice, the superconductivity on the honeycomb system should be weaker than high T_c cuprates. It is interesting to see if this state can be realized in experiment.

This work is supported by NSFC Grant No. 10774187 and National Basic Research Program of China No. 2007CB925001 and No. 2010CB923004. The author is grateful for the discussions with Fan Yang and Cenke Xu.

APPENDIX

In this appendix, we present the mean field spinon dispersion of the chiral d-wave RVB state on honeycomb lattice for some typical values of Δ/χ. The result is shown in Fig.15.

[1] Z. Y. Meng, T. C. Lang, S. Wessel, F. F. Assaad, and A. Muramatsu, Nature 464, 847(2010).
[2] S. Moehlecke, Y. Kopelevich, and M. B. Maple, Phys. Rev. B 69, 134519 (2004).
[3] R. R. da Silva, J. H. S. Torres, and Y. Kopelevich, Phys. Rev. Lett. 87, 147001 (2001).
[4] K. S. Novoselov, A. K. Geim, S. V. Morozov, D. Jiang, Y. Zhang, S. V. Dubonos, I. V. Grigorieva, and A. A. Firsov, Science 306, 666 (2004).
[5] G. Baskaran, Phys. Rev. B 65, 212505 (2002).
[6] A. M. Black-Schaffer and S. Doniach, Phys. Rev. B 75, 134512 (2007).
[7] B. Uchoa and A. H. C. Neto, Phys. Rev. Lett. 98, 146801 (2007).
[8] Y. J. Jiang, D. X. Yao, E. W. Carlson, H. D. Chen and J. P. Hu, Phys. Rev. B 77, 235420 (2008).
[9] S. Pathak, V. B. Shenoy, and G. Baskaran, Phys. Rev. B 81, 085431 (2010).
[10] I. Affleck and J. B. Marston, Phys. Rev. B 37, 3774(1988).
[11] D. P. Arovas and A. Auerbach, Phys. Rev. B 38, 316(1988).
[12] G. Kotliar and J. Liu, Phys. Rev. B 38, 5142 (1988).
[13] P.A. Lee, N. Nagaosa and X-G Wen, Rev. Mod. Phys. 78, 17 (2006).
[14] Y.M. Lu and Y. Ran, arXiv:1005.4229.
[15] X. G. Wen, Phys. Rev. B 65, 165113(2002).
[16] D. A. Ivanov and T. Senthil, Phys. Rev. B 66, 115111 (2002).
[17] Tao Li and Hong-Yu Yang, Phys. Rev. B, 75, 172502(2007).
[18] H. Mosadeq, F. Shahbazi and S.A. Jafari, arXiv:1007.0127.
[19] S. Yunoki and S. Sorella, Phys. Rev. B 74, 014408 (2006).
[20] Tao Li, arXiv:1101.0193.
[21] Tao Li, EPL 93, 37007(2011).
[22] We are grateful to Cenke Xu for pointing out this observation to us.

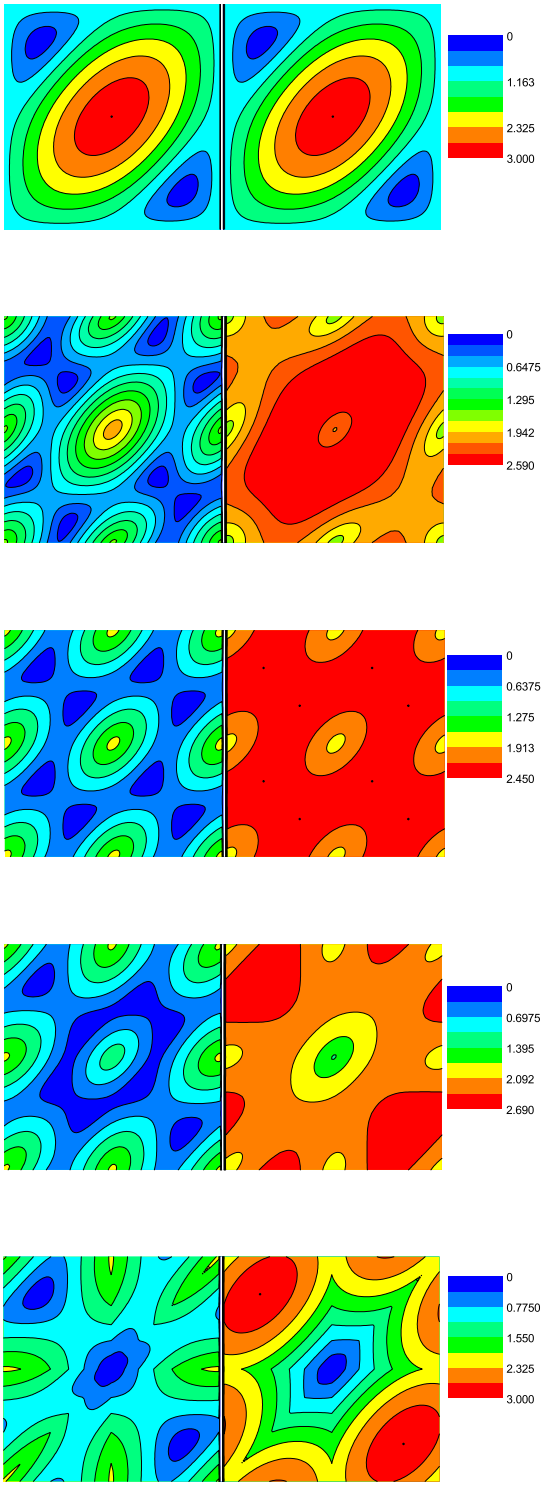

FIG. 15: The evolution of the mean field spinon dispersion as a function of Δ/χ. From top to bottom are the results for $\Delta/\chi = 0$, $\Delta/\chi = 1$, $\Delta/\chi = \sqrt{2}$, $\Delta/\chi = 2$ and $\chi/\Delta = 0$. The value of χ and Δ are normalized so that $\chi^2 + \Delta^2 = 1$. The lower branches(E_k^-) are plotted in the left panel and the upper branch (E_k^+) are plotted in the right panel.